The Role of Point Defects in the Luminescence Processes in Inorganic Solids and Phosphor Development

The Role of Point Defects in the Luminescence Processes in Inorganic Solids and Phosphor Development

By

Arunachalam Lakshmanan

Cambridge
Scholars
Publishing

The Role of Point Defects in the Luminescence Processes in Inorganic Solids and Phosphor Development

By Arunachalam Lakshmanan

This book first published 2025

Cambridge Scholars Publishing

Lady Stephenson Library, Newcastle upon Tyne, NE6 2PA, UK

British Library Cataloguing in Publication Data
A catalogue record for this book is available from the British Library

ISBN: 978-1-0364-1809-0
ISBN (Ebook): 978-1-0364-1810-6

TABLE OF CONTENTS

ABOUT THE AUTHOR

Dr. Arunachalam Lakshmanan obtained his Bachelor and Master degrees in Physics with a specialization in Spectroscopy from Annamalai University in 1968 and 1970. He joined the Thermoluminescence Dosimetry (TLD) group at the Division of Radiological Protection, BARC, Trombay, in 1971. That was the time when focus was shifting from film to TLD for radiation monitoring. He and his senior colleagues were instrumental in the synthesis of $CaSO_4$:Dy TL phosphor and in the design of the present TLD badge in 1975. In view of its high sensitivity, reliability, accuracy, and ruggedness, DAE is using it for countrywide radiation monitoring in nuclear installations as well as medical and other industries. He obtained his PhD in the field of TLD in 1980 from Bombay University under the guidance of Dr. K. G. Vohra. During 1982-84, he served as a Scientific Associate at CERN, Geneva, Switzerland, and as an AVH Fellow at the University of Wuppertal, Germany. His other foreign tenures include visiting professorships at various universities in Japan, Korea and France. He published a number of research papers in reputed international journals in the fields of radiation dosimetry of X-and γ rays, UV radiation and high LET radiations such as pions, neutrons etc. Dr. Lakshmanan's work on sensitization and supralinearity of $CaSO_4$:Dy, LET dependence of LiF:Mg,Ti and CaF_2:Tm based on multi-hit traps, reusability of Teflon based TLD, light induced fading, measurement of new ICRU quantities with $CaSO_4$:Dy TLD badge, irradiation temperature dependence studies in LiF, high level gamma dosimetry using TLDs and

neutron dosimetry based on sulphur activation are some of his pioneering work carried out at BARC.

In 1990, Dr. Lakshmanan got transferred to the Health and Safety Lab at IGCAR, Kalpakkam and became the head of Radiation Dosimetry Section. He widened his interest to optical absorption (OA) photoluminescence (PL) and photostimulated luminescence (PSL) studies, apart from the development of new TL phosphors. His review of the PL and TL Processes in Rare Earth doped $CaSO_4$ in the Progress in Materials Science journal issue l44 (1990) 1-187 has highlighted the pivotal role of Dy and Tm dopants in the TL process. Two new routes of synthesis of high sensitive $CaSO_4$:Dy phosphor were developed by him. A notable outcome of his research work at IGCAR was the development of a new phosphor based on $CaSO_4$:Ag,Tm with a TL peak near 400^0C for radiation dosimetry at high temperatures in reactor environments. His prediction that Ag^+ acts as hole trap has been subsequently confirmed with ESR studies. The PL of F_2 and F_3^+ centres in LiF and its applications in neutron and high level gamma dosimetry, high temperature effect on $CaSO_4$:Dy Teflon discs and the development of Quantum Cutting phosphor based on $CaSO_4$:Tb,Na are some of his important contributions. The proper identification of electron-hole traps in the BaFBr:Eu^{2+} X-ray storage phosphor by him has resulted in the photostimlated luminescence (PSL) process which restore its virgin status after PSL readout to enable its reusability for x-ray imaging in hospitals. He guided a few of his colleagues at IGCAR in obtaining their PhD degrees. A novel method of peaceful dissolution of sodium metal (used as a coolant in fast reactors) using an aqueous solution of Epsom salt with eco-friendly by products developed by him is a breakthrough in the fields of sodium chemistry and fast reactor safety. This solution spray is capable of quenching sodium fire and neutralizing sodium aerosol. This work is now internationally recognized and is considered a superior technique to all other existing techniques for removing efficiency in an eco-friendly way sodium metal from all types of components.

On superannuation from IGCAR in 2007, he joined the Saveetha Engineering College, Chennai as a research professor and is presently the Dean, R & D in that college. He is a recognized guide for PhD at Anna University and is guiding a number of faculty members in the field of luminescence. A new TL phosphor based on $CaSO_4$:Zn,Mn and a new co-precipitation route for the synthesis of $BaSO_4$:Eu^{2+} have been developed recently by his group. These studies have elucidated the role of anion interstitials and anion as well as cation vacancies in their luminescence

process. For the first time in India, recycling of PTFE scrap has been successfully carried out by him under a DSIR sponsored research project. The excess energy released during sodium metal dissolution in a dilute aqueous Epsom solution was recently attributed by Dr. Lakshmanan to the Hawking radiation on evaporation of micro black holes formed due to high energy proton-proton collisions in the H_2^{2+} species trapped in condensed matter during sodium metal dissolution in a dilute aqueous Epsom salt solution[@]. A confirmation of this novel idea would lead to the discovery of an infinite source of green energy with water as fuel, sodium metal and Epsom salt as catalysts.

@ Arunachalam Lakshmanan. Insights in Nuclear Enegy, Science and Engineering 2024, 2(1):005-013

ABSTRACT

Specialists working with lighting in different disciplines, such as display and imaging devices in medical institutes or scintillators in particle accelerators and stimulated luminescence phosphors like BaFBr:Eu, LiF and $CaSO_4$:Dy/$BaSO_4$:Eu in nuclear installations, will not only be keen on understanding the luminescence process but will also be interested in developing them for newer applications such as 3D x-ray imaging, high energy particle detection and electronic data storage. New sensitive phosphor development requires an understanding of material development as well as the role of point defects (vacancies, interstitials and impurity atoms/ions) in solids which is not readily available in the literature. While doping of impurities in suitable inorganic solids suffices for obtaining bright fluorescence, the creation of suitable electron-hole traps is necessary in stimulated luminescence, a fact usually not highlighted properly. Hence, the different luminescence processes remain largely unexplained so far. This book is intended to bridge this gap and enlighten readers from different disciplines about the intricacies of phosphor development and luminescence phenomena. *It will serve as a source book on some of the technologically important stimulated luminescence phosphors.*

GRAPHICAL ABSTRACTS

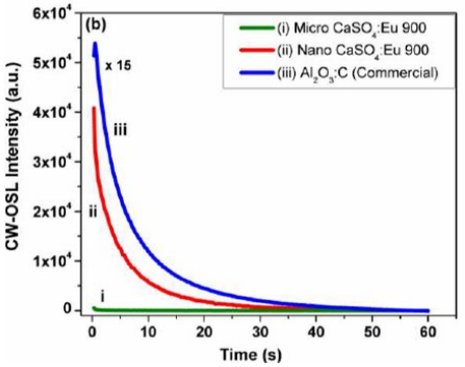

I. CW-OSL curves of various phosphors exposed to 1 Gy from Sr^{90}/Y^{90} beta source. (i) Microcrystalline CaSO4:Eu@900, (ii) Nano CaSO4:Eu@900, (iii) Commercial α-Al2O3:C. The ordinate is to be multiplied by the numbers at the curves to get the relative intensities **[Ma 20].** CaSO4:Eu microscrystalline powder prepared by conventional recrystalline (100-200 μm) technique gives considerably less OSL than the semi micro phosphor prepared by co-precipitation and annealed at 900^0C (2-4 μm). The reason for this might be attributed to enhanced contribution to OSL from surface traps. This is perhaps the first confirmed evidence of importance of microcrystalline phosphors in optically stimulated luminescence.

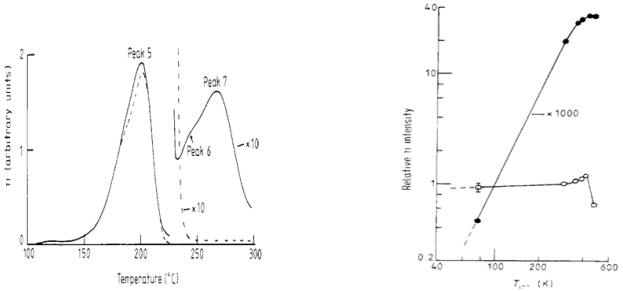

II. **Left -** A typical TL glow curve of LiF:Mg,Ti chips after ^{60}Co γ-irradiation at 20^0C (-) and at *77* K (---). γ-dose = 18 Gy. For both the glow curves, the TL intensities beyond 220^0C are magnified by a factor of 10 **(La 85). Right -** Relative

TL intensities of peak ***5*** (0) and peak ***7 (●)***in LiF:Mg,Ti chips as a function of irradiation temperature *T(K).* All TL intensities are normalised with peak 5 TL at T_{irr} = 293 K **(La 85).** In LiF:Mg,Ti dosimeters, γ- irradiation at 77 K reduces the TL intensities of peaks 7 (260^0 C) and 10 (450^0C) drastically whereas the TL intensity of dosimetry peak **5** (200^0 C) remains nearly the same as that after irradiation at room temperature (RT) as shown. This implies that electron-hole traps are involved in the formation of peak 5 during irradiation, as proposed by Mayhugh **[Ma 70]** but interstitial migration is involved in the formation of traps giving rise to peaks 7 and 10 as proposed by Sagastibelza and alvarez Rivas **[Sa 81].** Thus, LiF:Mg,Ti is perhaps the only TL phosphor in which both electron-hole process as well as interstitial-vacancy process operate simulataneously.

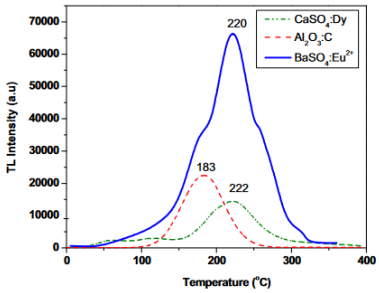

TL glow curves

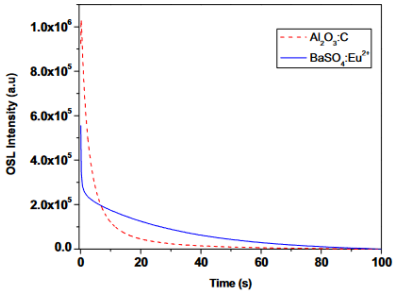

OSL decay curves

III. The $BaSO_4$:Eu,X made by the Japanese group **[Ok 86]** is 11 times more sensitive than $CaSO_4$:Dy to ^{60}Co γ-radiation. Amongst the TL phosphors reported so far in the literature, $BaSO_4$:Eu is the most sensitive one for γ-radiation. Its TL resonse to 247 nm UV rays is also the highest among the available large band gap TL phosphors which makes it as a useful TL phosphor for ionizing as well as nonionizig radiation dosimetry **[Bh 97].** Its OSL sensitivity is 75% of the commercial Al_2O_3:C which means it can be used for radiation dosimetry using OSL as well **[Bh 14].** However, its recipe is largely unknown despite the lapse of 38 yrs sincs its discovery. The reported enhancement in TL sensitivity of $BaSO_4:Eu^{2+}$ with P codoping by Shinde et al. **[Sh 94]** could not be reproduced and is not consistent with the principle of charge compensation. Other reports and our investigation indicate that the cooping of P in fact quenches the TL sensitivity of $BaSO_4$:Eu due to the conversion of Eu^{2+} to Eu^{3+}. The sensitizer X used to enhance the TL sensitivity of $BaSO_4:Eu^{2+}$,X by Okamoto **[Ok 86]** appears to be different from phosphorous. The TL sensitivity of the $BaSO_4$:Eu,X TL powder is almost constant over a Eu concentration region of 0.1 to 1.0 mol%. While the TL light yield of LiF(NTL-500) decreased rapidly with decreasing grain size, the TL of $BaSO_4$:Eu powder was almost constant up to several tens of μm. These peculiar results indicate that it is a new kind of TL phosphor unlike other ones all of which show an increase in TL sensitivity with grain size and activator concentration.

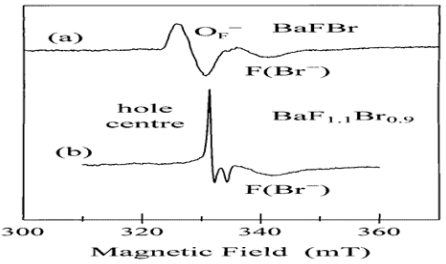

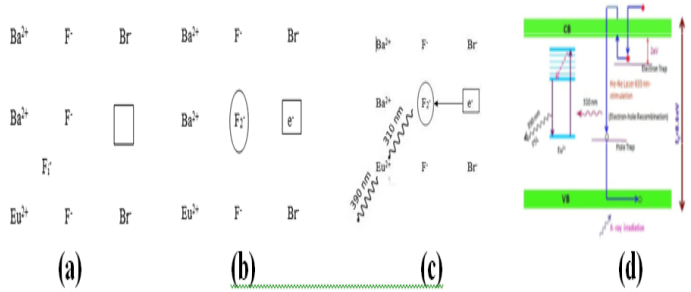

IV. **Top -** EPR spectra from nonstoichimetric fluorine excess BaFBr:Eu showed the F(Br$^-$) line and the signal due to a new H-type hole centres formed in the F$^-$ sublattice **[Sc 98].** This ESR study paved the way for identifying the hole traps in fluorine excess BaFBr:Eu^{2+}. **Bottom Left** - Before x-irradiation (a), After x-irrdiation (b) and During PSL readout (c). F(Br$^-$) electron centres and H(F2-) type hole centres created on x-irradiation as per the model proposed by us. **Right –** PSL mechanism proposed by us **[La 08a, Sa 22].** This involves liberation of F(Br$^-$) electrons followed by recombination with holes trapped at the above H- type hole centers and the recombination energy decay under Eu^{2+} luminescence. This process restores the crystal to virgin state once the PSL process is over paving the way for its reuse.

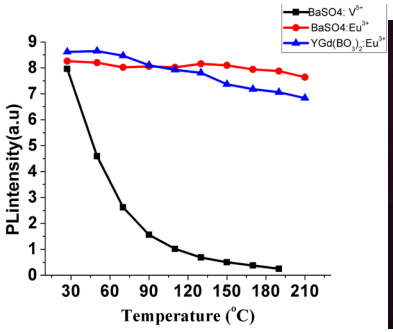

(a)

(b)

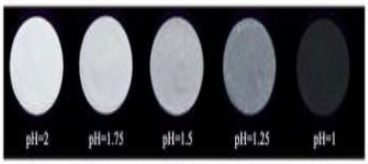

Photographs of SiO_2-coated $BaSO_4$:3%V^{5+} after immersion in HCl at pH= 2-1

(c)

V. Luminescence in $BaSO_4$:V^{5+}, Eu^{3+} Ba^{2+} SO_4^{2-} Eu^{3+} VO_4^{3-} **(a)** Thermal quenching of V^{5+} and Eu^{3+} PL emission in $BaSO_4$: V^{5+} (3 %), Eu^{3+}(2 %) sintered at 1000°C for 2h in air. This phosphor was developed recently in our lab. 495 nm V^{5+} emission (■) under 350 nm excitation, 619 nm Eu^{3+} emission (●) under 398 nm excitation and commercial YGd $(BO_3)_2$:Eu^{3+} (▲) emission under 398 nm excitation. While vanadium emission shows large thermal quenching, Eu^{3+} emission intensity remains same in the excitation temperature range 25-200^{0}C. **(b)** Red emission from $BaSO_4$:V,Eu (λ_{exc}-398 nm). The Eu^{3+} red emission centered at 619 nm does not show thermal quenching and its PL intensity is enhanced due to charge compensation**.** Its emission intensity is comparable to that of commercial red phosphors used in white LEDs. The ratioof Eu^{3+} to V^{5+} fluorescence emission intensity increases with temperature in the range 30- 180^{0}C which can be used as a *noncontact luminescence thermometry* [Va 24]. (c) Photographs of PL emission from SiO_2 coated $BaSO_4$:V^{5+} (3%) after immersion in HCl solution. The V^{5+} ions is proposed to be situated on the grain surface of $BaSO_4$. The drastic decrease in the PL intensity of vanadium with a decrease in pH (increase in the acidity) of gastric solution (due to release of V into solution with reduced pH) is suggested for *biomedical applications* **[Ch 24]**. This study reveals the importance of luminescence from grain surface.

PREFACE

Despite the widespread use of optically and thermally stimulated luminescence (OSL/TSL) phosphors for various applications, a detailed understanding of their basics, i.e., excat identification of electron traps, hole traps, radiolysis processes, generation of interstitials and vacancies, charge carriers released during stimulation, their recombination process, and the mechanism of energy transfer to activators, is lacking. There are three common types of defects (imperfections) in a crystal lattice: (a) a vacancy or missing atom, (b) a dislocation or misaligned row of atoms (c) grains or regions of atoms with differing crystal orientation. Point defects in solids refer to vacancies, interstitials, and impurity atoms/ions. Dislocations are examples of linear defects in which lines of ions are missing in an otherwise perfect array of ions. As far as the luminescence process is concerned, point defects play the vital role. They are created during phosphor synthesis: (i) through aliovalent dopants (eg.,cation vacancies created by Dy^{3+} doping in $CaSO_4$) or by nonstoichiometry e.g., Fluorine rich BaFBr:Eu^{2+} or by partial thermal decomposition process and crystalline phase change (e.g., $CaCO_3$ and $CaSO_4$), (ii) change in valency of dopant during X-irradiation e.g., redox process involving $Eu^{3+} \leftrightarrow Eu^{2+}$ or $Ag^{+} \leftrightarrow Ag^{2+}$ dopant in $CaSO_4$ host lattice and (iii) through radiolysis process during irradiation (e.g., alkali halides like LiF). In few instances, dislocations are reported to act as traps. For exampe, the TL found in LiF is reportedly caused by the recombination with vacancy centres (F, Z_2) of interstitial halogen atoms thermally released from traps such as impurities and dislocations in conflict with the commonly explained in terms of a model proposed in which the mobile entities are electrons and holes.

Prima facie, the difference between the optical *excitation* used to excite electrons from the ground state of an activator to excited states in fluorescence (also known as photoluminescence or PL) measurements usually does not involve pre-irradiation. This must be distinguished from *stimulated luminescence*. In the latter case, electrons and holes are usually created during irradiation by ionizing radiation and get trapped at metastable traps, their number being proportional to the radiation dose received. Stimulated luminescence, either by optical or thermal means involves the liberation of trapped electrons from traps and their recombination with holes in a crystal. The luminescence intensity vanishes

in this case, once the e-h recombination process is complete, while in PL, the luminescence lasts as long as excitation persists. Radiophotoluminescence (RPL), in which PL occurs after X- or γ-irradiation is an exception. RPL occurs from defects (e.g., F-aggregate centres in LiF created during irradiation by radiolysis) or radiation induced valence change in activators such as $Eu^{3+} \rightarrow Eu^{2+}$ or $Sm^{3+} \rightarrow Sm^{2+}$ in $CaSO_4$ or $BaSO_4$ hosts. Recently, intense RPL capable of measuring very low levels of radiation doses has been reported even in undoped materials such as $CaSO_4$, Li_2CO_3, Na_2CO_3 and K_2CO_3. The defects responsible for intense RPL in undoped $CaSO_4$ appear to have been generated during the phase change and decomposition at 1200˚C (No RPL is detected in $CaSO_4$ sintered at 1000˚C). The role of flux, if any in this RPL phosphor synthesis is, however, not clear. The RPL intensity is dose dependent and can be read again and again. The RPL efficiency of undoped $CaSO_4$ has been reported to be better than that of RPL from commercial Ag-activated phosphate glass used in radiation monitoring. It could measure dose levels as low as 400 μGy (40 mrad). If confirmed, the RPL from undoped $CaSO_4$:Dy can even be used for individual monitoring, thereby posing a serious competitor to the presently used TLD/OSL systems. It can also be used as an integrating dosimeter without the need to erase the signal after each use. The defect centres causing RPL can be destroyed only after the post-irradiation annealing treatment at a higher temperature, which resets the crystal to virgin state. The understanding of the relationship between point defects and different luminescence processes is, however, essential in the development of technologically important TL/PSL/OSL and RPL materials such as BaFBr:Eu used for X-ray imaging and wide band gap semiconducting PSL phosphor materials tried recently in optical data storage, thermostimuated luminescent (TSL) materials such as LiF:Mg,Ti and $CaSO_4$:Dy used for radiation dosimetry, colour centre lasers and radiation imaging detectors.

The PL of Eu^{3+} (RE) ions occurs by (1) a direct excitation of Eu^{3+} ions through intraconfigurational $4f^6$–$4f^6$ absorption transitions, (2) charge transfer transitions from ligand to europium (III) ion or (3) an energy transfer of absorbed energy from a host to rare-earth (RE) ions. Among these, the $4f^6$–$4f^6$ transitions lead to low values of absorption cross-sections because they are forbidden from the viewpoint of quantum mechanics. The wide band of the $O^{2-} \rightarrow Eu^{3+}$ charge–transfer transition has high intensity and is located at ~225–300 nm for many oxide compounds. However, the absence of cheap semiconductor chips with intensive radiation at this short wavelength makes excitation through the $O^{2-} \rightarrow Eu^{3+}$ mechanism inconvenient for LED applications.

The luminescence processes of luminescent materials can be divided into four main types: long persistent luminescence, down-conversion luminescence, up-conversion luminescence, and quantum cutting luminescence. Unfortunately, almost no quantum cutting luminescent nanomaterials are suitable to fabricate optical and optoelectrical data storage because of the shortage of nanomaterials with visible quantum cutting luminescence and sensitive near-infrared light response materials. Therefore, only three of the luminescence types are used for fabricating optical data storage (ODS) systems. On account of the latest achievements, OSL-based optical data storage may be the ideal option to develop high-density and high-capacity optical data storage devices.

The present book will highlight the recent progress made in understanding the luminescent processes that stimulate luminescence materials such as BaFBr:Eu based X-ray storage phosphors, rare earth doped $CaSO_4$ TL phosphors and optoelectronic data storage based on luminescent nanomaterials. leading to new applications. Specifically the role of oxygen impurities as hole traps in the PSL process of stoichiometric BaFBr:Eu^{2+} has been ruled out by the author's low temperature studies involving PL, TL and XIL (X-ray induced luminescence) in oxygen contaminated phosphor. The role of fluorine ion interstitials as hole traps in non stoichiometric BaFBr:Eu and bromine vacancies created during crystal growth as electron traps, along with a comprehensive PSL mechanism proposed by the author, explains for the first time how it gets reset once the PSL process is complete. In hospitals the imaging plate is reused thousands of times. The role of monovalent and divalent co-dopants in BaFBr:Eu which also serve as flux has been highlighted in our recent studies. New TL phosphors based on $CaSO_4$:Ag,Dy/Tm developed by the authors group for radiation measurements in high temperature environments, the dramatically opposite effect of codopant such as Zn on the TL glow curves of $CaSO_4$:Dy and $CaSO_4$:Mn and a new simplified recipe for $CaSO_4$:Dy based on coprecipitation in acid media developed for the first time by the author that yields superior TL characteristics than the conventional recrystallization method will be highlighted. The pioneering electron paramagnetic resonance (EPR) work in nonstoichiomeic fluorine excess BaFBr:Eu storage phosphor which was instrumental in identifying its hole traps and the EPR work that identified for the first time the electron and hole traps in $CaSO_4$:Ag,Dy will be described. A recent study has identified oxygen interstitial ions as hole traps and sulphate ion vacancies (F^+ centres) as electron traps in $CaSO_4$:Dy. Intense RPL from undoped $CaSO_4$ exhibiting PL emission at 690 nm on 590 nm excitation discovered recently is explained well with the above defect structure on the basis of F centre fluorescence. The decrease in TL sensitivity on prolonged annealing at 400^0 C and its restoration on annealing at 700^0 C observed

in the widely used $CaSO_4$:Dy phosphor could also be explained well with the above identification. While annealing near 400^0C destabilizes the oxygen defect, possibly by way of their thermal migration to F-centres, the high temperature sintering at 700^0C restores its defect structure. Thermal annealing much below 400^0C does not affect the TL since the activation energy required to migrate the interstitial oxygen ions is not achieved at lower temperatures. As a result of this study, it was concluded that the post-irradiation annealing treatment in the temperature range of 600 to 650^0C could be the best alternative to the previously mentioned 400^0C treatment for annealing and re-use of $CaSO_4$:Dy phosphor powder. *But for the understanding of point defects, these results would have gone unexplained.*

Current X-ray imaging technologies involving flat-panel detectors have difficulty in imaging three-dimensional objects because the fabrication of large-area, flexible, silicon-based photodetectors on highly curved surfaces remains a challenge**.** Persistent luminescence lasting for several days after X-irradiation has been used earlier to obtain high resolution imaging of curved objects**.** Imaging with a resolution greater than 20-line pairs per mm and optical memory longer than 15 days has been reported. Conventional x-ray imaging plates based on PSL from BaFBr:Eu exhibit only 5 lines per mm resolution. Recently, the use of a flexible film of $BaSiO_3$:Eu^{2+} to demonstrate real-time X-ray imaging and achieve time-delayed X-ray imaging of curved objects, such as flexible circuit boards using TL from deep traps giving rise to a peak around 250^0C has been reported for the first time. After X-irradiation, the flexible film was placed on a heating table at 220°C to obtain the TL for image acquisition, which looked promising**.** Time-delayed X-ray imaging cannot be used for real time applications such as baggage scanning in airports. So further progress using TL imaging is worth making.

A large enhancement in TL intensity on UV and γ-irradiation has been reported in $BaSO_4$:Eu^{2+},P^{3+} phosphor perhaps due to the transfer of electrons from the PO_4^{3-} complex to anion vacancies. Suppression of these anion vacancies by $Eu^{2+} \rightarrow Eu^{3+}$ oxidation which occurs easily during phosphor preparation with phosphotous codoping, however, quenches the TL**.** So it has become a challenge to synthesize $BaSO_4$:Eu to obtain a high TL sensitivity to X as well as UV radiations. A $BaSO_4$:Eu^{2+} phosphor which yields least TL but high PL with potential applications for scintillation applications has, however, been synthesized by us recently**.**

The early start and intense research on alkali halides, especially LiF, LiF:Mg,Ti, LiF:Ti and LiF:Mg,Cu,P used in radiation dosimetry, colour centre lasers and imaging has led to several publications. This review will elucidate the progress made in the role of point defects in stimulated luminescence processes in LiF and RPL applications. Extensive optical absorption (OA) studies using single crystals of LiF (undoped), LiF:Ti and LiF:Mg,Ti supplied by Harshaw chemical co., USA with different doses of γ- and thermal neutron radiation, different irradiation temperatures followed by TL studies after partial post-irradiation annealing studies carried out by the author have led to the correlation of different defect centres with the respective OA bands and TL peaks. It was suggested that while the TL peaks in other alkali halides arise due to interstitial-vacancy recombination, LiF alone cannot be different. Our pioneering low temperature irradiation studies resolved this controversy amicably. The study revealed that in dosimetry grade LiF (LiF:Mg,Ti), the defects causing TL peaks between RT and 230^0C (up to peak V) arise due to electron-hole recombination, and the high temperature TL peaks above 230^0C (mainly 270^0C and 400^0C peaks) are caused by interstitial-vacancy recombination. In undoped and Ti doped LiF, however, all TL peaks arise due to interstitial-vacancy recombination, as with other alkali halides. The dependence of the luminescence efficiency of different LiF phosphors on LET (ionization density) of incident radiation and RPL from F-aggregate centres and their applications in high dose dosimetry will be elaborated. Our recent work on the application of microdosimetric concepts in $CaCO_3$:Dy and $CaCO_3$:Ce and the importance of the charge state of the defects in secondary electron track interaction at high γ-doses will be highlighted.

While the growth of nanophosphors and quantum dots has been phenomenal in display applications, their growth in doped crystals is very minimal. A recent study on $CaSO_4$:Eu however, indicates that microscrystalline powder prepared by conventional recrystalline (100 -200 μm) technique gives considerably less OSL than the semi micro phosphor prepared by co-precipitation and annealing a sample at 900^0C (2-4 μm). The reason for this might be attributed to the enhanced contribution to OSL from surface traps. This is perhaps the first confirmed evidence of the importance of nanophosphors in optically stimulated luminescence. But the situation is different in TL. Since TL is a volume phenomenon, nanophosphors usually exhibit TL peaks at low temperatures with reduced TL intensity than those of the bulk phosphors.

Recently the importance of surface traps (eg., $BaSO_4:V^{5+}$) in photoluminescence and its applications in measuring the acidity of gastric solutions has come to light. $BaSO_4:V^{5+},Eu^{3+}$ with a good thermal stability developed in our group is a promising new red phosphor for improving the color rendering of white LEDs. The ratio of Eu^{3+} to V^{5+} fluorescence emission intensity in it increases with temperature in the range 30-180^{0}C which can be used as a noncontact luminescence thermometrey. The continually growing interest in luminescent thermometry (LT) emerges from the fact that this technique, due to its numerous advantages has a potential to become an alternative to conventional methods of temperature sensing. In addition, some of its features like fast response, non-contact operating mode and the small size of the temperature sensor, make LT a useful tool that provides an unrivalled opportunity of temperature mapping with submicrometer spatial resolution.

The space coverage on luminescence of divalent metal sulphate and silicate materials in this book is more than twice that of BaFBr:Eu or LiF. This is due to the ease of production of a variety of defects both during crystal growth and during irradiation, causing luminescence in the former class of materials.

CHAPTER 1

DEFECTS AND OSL PROCESS IN BAFBR:EU PHOSPHOR

Computed radiography (CR) uses storage phosphor imaging plates for digital imaging. Absorbed X-ray energy is stored in crystal defects. In read-out, the energy is set free as light photons upon optical stimulation. Several storage phosphor families have been investigated and developed. But only some materials made it to the commercial stage, while others did not. In this chapter, the recent progress made in the optically stimulated luminescence (OSL) mechanism of the current commercial storage phosphor, BaFBr:Eu^{2+} is discussed. The dynamic range for image formation in BaFBr:Eu of over 5 orders of magnitude makes it superior to conventional x-ray films for many applications in medicine, crystallography, and biochemistry **[Ko 91, La 94a, Le 11].**

In contrast to X-ray scintillators, where the X-ray energy is directly converted into visible light, X-ray storage phosphors store the radiation image in proportion to its intensity distribution in a storage phosphor screen. During the read-out process, the X-ray storage phosphor image plate is optically stimulated pixel by pixel and line by line by means of a laser beam, e.g., a He-Ne laser (632.8 nm) for the commercially used BaFBr:Eu^{2+} phosphor screen. The PSL light is collected globally with a waveguide and detected by a photo multiplier. The stimulation light is cut off by means of an appropriate optical filter combination, which is placed between the waveguide and the photomultiplier. The detected luminescence intensity during stimulation of a pixel is a measure of the absorbed X-ray dose in that pixel. The analogue signal of the photomultiplier is converted by an analogue/digital (A/D) converter to a digital signal. The scanning procedure is carried out by moving the laser. The ability to detect the calcifications with digital images (ROC area = 0.871 ± 0.066) with CR was equivalent to conventional mammography (ROC area = 0.866 ± 0.075) despite the lower spatial resolution **[Oe 88].**

The main experimental method used to analyse the nature of the generated electron and hole trap centres, which are the basis of the information storage and read-out processes, is electron paramagnetic resonance (EPR), because electron and hole trap centres are paramagnetic before they recombine in the PSL process. For detailed defect investigations, electron nuclear double resonance (ENDOR) is also needed. However, because of the low defect concentration, conventional EPR and ENDOR are often not sensitive enough. Therefore, optically detected EPR and ENDOR techniques have to be applied. Their basis is the detection of changes in the magnetic circular dichroism of optical absorption (MCDA) induced by EPR/ENDOR transitions. Although the principle of information storage and read-out mechanism is simple, it is not clearly known how the recombination energy is transferred to the activator Eu^{2+} which emits at 3.18 eV (390 nm). The PSL decay time is 750 ns. After many years of thorough research and optimisation, BaFBr:Eu^{2+} has already reached a very high level of performance **[Le 11].** However, there is still space for some improvements, such as e.g., a better conversion to OSL-active centres, a higher stability of the OSL active centres, and a better erasability of the generated defects after the read-out process. The spatial resolution can probably not be improved. The peak wavelength of OSL emission and stimulation spectra for various photostimulable storage phosphor materials and their application in radiation monitoring have been reviewed by Nanto **[Na 18a].** Commercial computed radiography (CR) phosphors today are phosphors of the BaFX:Eu^{2+} family and CsBr:Eu^{2+}. Both materials have a relatively high density of about 5 g/cm^3 and contain an element with a K-edge between 35 and 40 keV, which matches well with the X-ray spectra used in general radiography. Alternatives to BaFBr:Eu phosphors, which can be used for imaging, have been listed by Leblans et. al **[Le 11]. Table 1.1** compares the characteristics of some of these phosphors.

SEM image of BaFBr:Eu commercial storage phosphor powder shows particles with a median particle size of 2 to 15 µ. Individual particles may be sub-µ or as large as 30 to 40 µ as seen in **Figure 1.1.** The morphology of the phosphor crystals in the CR imaging plates has been reported to have a very significant impact on its performance. The light-guiding character of the crystals in needle phosphor-based imaging plates (NIP) leads to a large benefit over phosphor-based imaging plate (PIP). It allows the use of much thicker phosphor layers in general radiography that have at least two times higher X-ray absorption. The higher light transparency further leads to a higher system gain, and the IP's are more homogeneous and lead to less screenstructure noise. It has been demonstrated that, for many general radiography applications, NIP leads to the same image

quality as PIP at 50% or less of the X-ray dose. CR with NIP offers the same image quality for most general radiography applications as direct radiography (DR) with a CsI:Tl^+ needle scintillator plate.

Table 1.1 [Le11]

PSL characteristics of In^+ and Ga^+ doped alkali halide storage phosphors in comparison with standard BaFBr:Eu^{2+}.

Phosphor	Stimulating laser wavelengtd (nm)	Peak PSL wavelengtd (nm)	Peak stimulation wavelengtd (nm)	CE pJ/mm^2/mR	SE µJ/mm^2
BaFBr:Eu^{2+}	633	390	550	20	16
BaFBr:Eu^{2+}	680	390	550	14	28
RbBr:In^+	680	490	700	2	25
RbBr:Ga^+	680	550	705	6	4
CsBr:In^+	680	504	700	3	23
CsBr:Ga^+	680	515	685	6	4

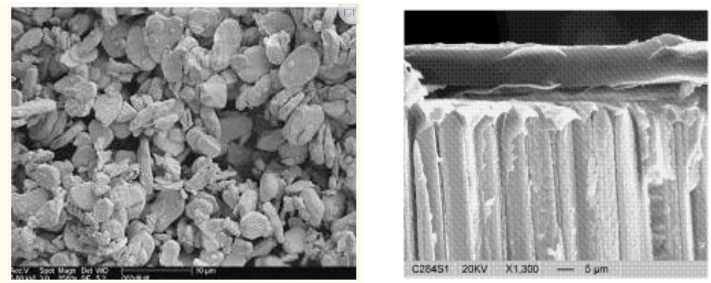

A B

Figure 1.1. (A) SEM image of BaFBr:Eu commercial storage phosphor powder **[Le 11].** Conversion efficiency (CE): the total energy of stimulated light per unit area and per unit of X-ray dose produced by the phosphor in pJ/mm^2/mR, Stimulation energy (SE): the laser energy per unit area required to release 63% of the stored energy in µJ/mm^2. **(B)** Image of needle shaped CsBr:Eu^{2+} storage phosphor **[Le 03].**

1.1. PSL Process in Stoichiometric BaFBr:Eu

X-irradiation generates F centres as electron trap centres. In BaFBr, which has the matlockite structure, two F centres are possible, F(Br^-) and F(F^-) centres, where electrons are trapped at Br^- vacancies or F^- vacancies, respectively. Their generation mechanism, however, is controversial. In order to form an F centre after creating electron–hole pairs by X- irradiation,

one either needs to have a halide vacancy present in the crystal or one must generate it during the radiation damage process. Hesse et al. **[He 09]** assumed that Br^- vacancies were already present in the material. However, no experimental evidence was given for this assumption.

In stoichiometric BaFBr:Eu, produced by firing stoichiometric mixtures of BaF_2 and $BaBr_2$ or by growing single crystals from the melt of such mixtures with the Bridgman method, all are contaminated with oxygen, irrespective of the manufacturer. All attempts to eliminate oxygen completely have failed. Very careful avoidance of oxygen could only reduce the oxygen contamination. Oxygen can be incorporated in many ways: It was found by EPR and ENDOR investigations as O^{2-} in the fluorine (O_F^{2-}) as well as in the bromine sublattice (O_{Br}^{2-}). Upon X-irradiation at temperatures below 120 K, $V_k(Br_2^-)$ centres and $F(Br^-)$ centres are formed, the latter being near to the O_F^{2-} centres. Above 120 K, the $V_k(Br_2^-)$ centres become mobile, react with the O_F^{2-} centres and form O_F^- hole trap centres. Above 200 K, the $F(Br^-)$ centres can diffuse away and become isolated.

In the author's investigation, there was no 480 nm PL emission from O_F^{2-} in the X-ray induced luminescence (XIL) from Fuji IP **[La 01a**]. So, there is no evidence for the presence of oxygen in Fuji IP. It is also not certain if it contains a stoichiometric BaFBr compound. To explain the PSL process, it was proposed that that the recombination between electrons and holes takes place via tunnelling and that a kind of "aggregate" between F centres, hole trap centres and the activator Eu^{2+} must be formed during X-irradiation, called triple aggregate centres. Tunnelling, however, requires a spatial correlation between the F centre and the activator. Direct evidence for a spatial correlation between F centres, O_F^- centres and Eu^{2+} was obtained with cross-relaxation spectroscopy using magneto-optical techniques. When bleaching into the F centre band, the number of F centres can be drastically decreased to practically zero, while that of the O_F^- centres is hardly affected: The decrease is at most by 20–30%. Hence, it is not very likely that the F centres are those active electron trap centres in the triple aggregates described above. On the other hand, it was found that the variation of the oxygen content influences the PSL intensity. A low oxygen content result in a low PSL intensity. Also, the stimulation energy needed for the read-out process is higher for oxygen-poor BaFBr. Thus, it seems that oxygen is involved in two ways in the PSL mechanism: It provides vacancies for the $F(Br^-)$ generation, and somehow it seems to influence favourably the photostimulation of the triple aggregate centres in that less stimulation energy is needed for read-out and a high PSL intensity result after short

stimulation. Thus, the role of oxygen in the PSL process of stoichiometric BaFBr:Eu^{2+} is far from clear.

The Eu^{2+} → Eu^{3+} redox model proposed originally, in which Eu^{2+} served as hole traps **[So 83, Ta 85]** was questioned by several authors since the EPR signal of Eu^{2+} did not change, nor could a change be observed in the Eu^{2+} luminescence upon prolonged X-irradiation. No Eu^{3+} fluorescence was observed in X-irradiated BaFBr:Eu^{2+}.

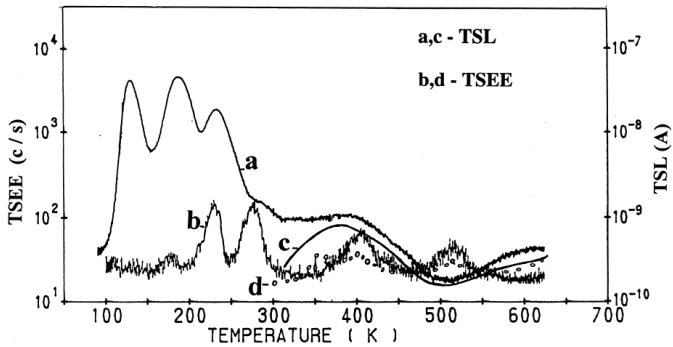

Figure 1.2. TSL (a), (c) and TSEE (b), (d) glow curves of BaFBr:Eu,O after X-irradiation at 98 and 295 K for 10 min (35 kV, 15 mA), respectively **[La 01a].**

1.2. Luminescence in BaFBr:O_F^{2-} and BaFBr:Eu^{2+}, O_F^{2-}

The author's investigation revealed that the presence of inadvertent oxygen impurities quenched the PSL in stoichiometric BaFBr:Eu^{2+} made from the physical mixture of BaF_2 and $BaBr_2$ by solid state firing at 850^0C in a nitrogen atmosphere for 3hrs **[La 01a].** A reason for this is the competition between O_F^{2-} and the hole centres which cause PSL in trapping the holes generated during X-irradiation. Nitrogen gas contaminated with oxygen could be a source of oxygen impurities in the above study. The PL and TL emission spectra of BaFBr (undoped) and BaFBr:Eu,O both containing inadvertent oxygen impurity are shown in **Figure 1.3(i).** On 254 nm excitation at RT, the broad PL emission band at 480 nm (due to O_F^{2-} centers) from BaFBr (undoped) and from BaFBr:Eu^{2+},O was very bright. Very little Eu^{2+} emission at 380 nm could be detected in the latter sample at 254 nm excitation. On 280 nm excitation, however, a bright Eu^{2+} emission at 380 nm was observed along with a relatively less intense 480 nm O_F^{2-} emission. In contrast to BaFBr:Eu^{2+},O, the Fuji IP exhibited bright PL at 400 nm due to

Eu^{2+} but little PL emission was seen in the 480 nm region. No Eu^{3+} PL was seen in BaFBr:Eu^{2+},O and in Fuji IP.

TL glow curves of BaFBr:Eu,O after X-irradiation at 98 K **(Fig.1.2 curve a)** showed three peaks below RT (130, 180, and 230 K), a shoulder near 290 K and one peak above RT (380 K). Following X-irradiation at RT **(Fig.1.2 curve c),** only the 380 K TL peak was seen. TL peaks below RT displayed emission around 480 nm characteristic of O_F^{2-} whereas the TL peak above RT displays 380 nm emission characteristic of Eu^{2+}. The TL glow curve of BaFBr undoped was found to be similar to that of BaFBr: Eu^{2+} except for the absence of the 380 K peak. The TSEE (thermally stimulated exoelectron emission) peaks are negligible in their intensities. The absence of TSEE would normally indicate the absence of electron motion in the conduction band during TSL which means that the electron-hole recombination could be through a tunnelling process.

Fig. 1.3(i) shows the PL emission spectra of BaFBr (undoped) and BaFBr:Eu,O for excitation at 254 nm and at 284 nm. **Fig.1.3 (ii)** shows that in the emission spectra of all the TL peaks in BaFBr (undoped), the 480 nm emission is dominant. An additional emission peak at 300 nm host (STE) emission characteristic of BaFBr host is also seen more prominently in the low temperature peaks. **Figure 1.3 (iii)** shows the simplified band model for O_F^{2-} center PL excitation at 5.2 eV and emission at 2.8 eV (a), V_k centre TL emission at 5.2 eV (b). V_k centre annihilation causes the TL glow peaks below 120 K but only O_F^{2-} luminescence results in this case due to energy transfer from V_k centers to O_F^{2-} ions as shown. TL emission at 2.8 eV from O_F^{2-} centres occurs due to the recombination of thermally released electrons from three perturbed F(Br-) centres corresponding to 130, 180, and 230 K TL peaks with the holes trapped at O_F^{2-} sites.

The XIL spectra of BaFBr: Eu^{2+},O are shown in **Fig. 1.4a.** At the highest X-irradiation temperature (643 K), the Eu^{2+} emission at about 400 nm as well as the intense black body emission at 800 nm, are seen. At 579 K, the Eu^{2+} emission occurs at about 390 nm but the black body radiation is nearly absent. For temperatures below 378 K, the Eu^{2+} emission peaks at 380 nm and the emissions at 480 nm (due to O_F^{2-}) and 575 nm (unidentified), as well as the 300 nm STE emission, build up at the expense of Eu^{2+} emission with decreasing X-irradiation temperature. At low temperatures (≤ 217.6 K), the 300 nm emission is more intense than all other emissions, indicating that during XIL, *oxygen impurity inhibits the energy transfer from STE to* Eu^{2+} *ions.* The XIL spectra of BaFBr (undoped) were found to be similar to those of BaFBr:Eu^{2+},O, except for

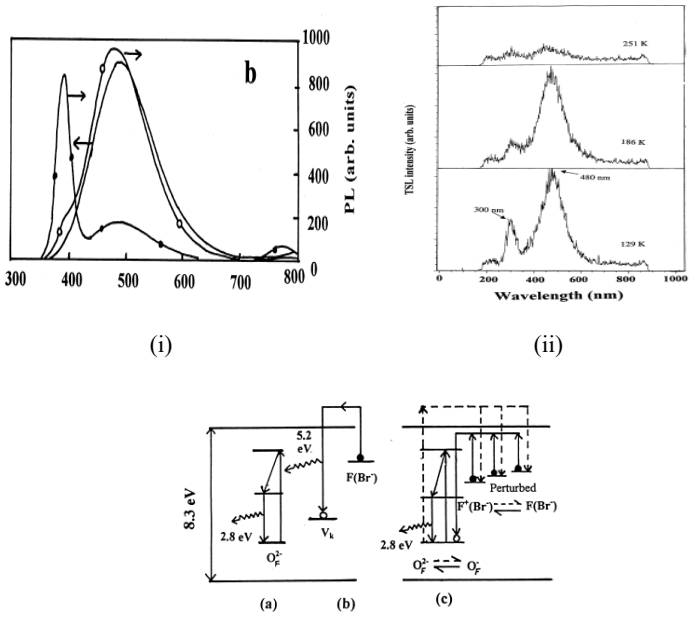

Figure. 1.3. (i) PL emission spectra of BaFBr (undoped) (--------) and BaFBr:Eu,O (--- O ---) and (---● ----) for excitation at 254 nm (--------) and (--- O ---) and 284 nm (---● ----).

Figure.1.3(ii). TL emission spectra of BaFBr:Eu,O at 130, 194, and 373 K.

Figure. 1.3(iii). (a) A simplified band model for O_F^{2-} center PL excitation at 5.2 eV and emission at 2.8 eV, (b) V_k center TL emission at 5.2 eV. (c) TL emission at 2.8 eV from O_F^{2-} centers due to the recombination of thermally released electrons from three perturbed F(Br-) centers corresponding to 130, 180, and 230 K TL peaks with the holes trapped at O_F^{2-} sites **[La 01a].**

the absence of the 380 nm Eu^{2+} emission. Only two emissions, a broad band with a peak emission in the region 450 nm (at 334 K) to 480 nm (at 83 K) and a relatively a sharp one at 300 nm could be clearly seen. Here again, the 300 nm emission builds up at low irradiation temperatures. The TL glow curve of the Fuji IP below RT was similar to that of BaFBr:Eu^{2+},O, but the TL peak above RT (as well as PSL) was much more intense in the Fuji sample. The TL emission spectra of Fuji sample in the temperature range 95 -290.5 K perhaps recorded for the first time,

are shown in **Fig. 1.4 b** clearly reveals the presence of two emissions, one peaking near 400 nm (characteristic of Eu^{2+}) and another unidentified broad peak around 450 nm. It is not clear if it is due to oxygen impurities. Interestingly, the XIL spectra of the Fuji IP showed only the 400 nm Eu^{2+} emission at all temperatures. The 450 nm emission was hardly visible. *The emission at 300 nm was not seen at all, indicating that an efficient energy transfer from the host to Eu^{2+} occurs in the Fuji IP.* In the PL and TL spectra, the Eu^{2+} emission in the Fuji IP occurs at 400 nm, whereas in BaFBr:Eu^{2+},O, it occurs at 380 nm. This is due to the presence of iodine in the Fuji IP. The addition of iodine is known to shift the photostimulation as well as the emission spectra of BaFBr:Eu^{2+} to the long wave length **[Mi 89].**

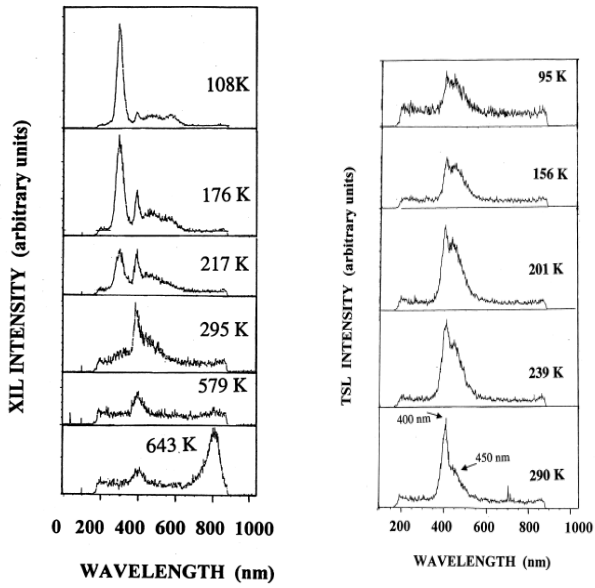

(a) (b)

Figure. 1.4a. X-ray induced luminescence (XIL) spectra of BaFBr:Eu^{2+},O at 108, 176, 218, 295, 579, and 643 K **[La 01a].**

Figure.1.4b. X-ray induced TL emission spectra of Fuji IP recorded at 95, 156, 201, 239, and 290 K **[La 01a].**

Thus, the above study reveals no evidence of oxygen contamination in commercial BaFBr:Eu^{2+} IP. Oxygen, if present, inhibits the energy transfer